Low-Temperature Controllable Calcination Syntheses of Potassium Dititanate

Ningzhong Bao
College of Chemical Engineering, Nanjing University of Technology, Nanjing, 210009, China

and

Research Laboratory of Hydrothermal Chemistry, Kochi University, Japan

Xin Feng and Xiaohua Lu
College of Chemical Engineering, Nanjing University of Technology, Nanjing, 210009, China

Liming Shen
College of Material Science and Engineering, Nanjing University of Technology, Nanjing, 210009, China

Kazumichi Yanagisawa
Research Laboratory of Hydrothermal Chemistry, Faculty of Science, Kochi University, Japan

DOI 10.1002/aic.10167
Published online in Wiley InterScience (www.interscience.wiley.com).

Thermodynamic calculations were used to estimate the free energy for reactions of anatase and TiO_2·nH_2O with K_2CO_3 to generate potassium dititanate at 25–1200°C, and the results showed that amorphous TiO_2·nH_2O with reaction activity higher than that of anatase can decrease the lowest generation temperature of potassium dititanate. The precise temperatures of 300°C for TiO_2·nH_2O and 500°C for anatase were determined by experiments. The crystal growth of potassium dititanate was studied experimentally. It was found that potassium dititanate hydrate is first formed from TiO_2·nH_2O at 300°C, and converts into $K_2Ti_2O_5$·0.35H_2O at 640°C. The dehydration of $K_2Ti_2O_5$·0.35H_2O occurs at 660–820°C, ending with the generation of $K_2Ti_2O_5$ single crystals at 820°C. Potassium dititanates with a diversity of morphologies, sizes, water contents, and crystallinities, showing various abilities for optical absorption/reflex, were fabricated from TiO_2·nH_2O under control, whereas only $K_2Ti_2O_5$ was prepared from anatase at 500–850°C, which indicate that reaction processes and properties of products are determined according to the type of reactants and the reaction temperature. © 2004 American Institute of Chemical Engineers *AIChE J,* 50: 1568–1577, 2004
Keywords: potassium dititanate, anatase, crystallinity, free energy, morphology

Introduction

Potassium dititanate is an important perovskite of the potassium titanate family (Bao, 2002a,b; Clearfield, 1988; Feng, 1999; Narita, 1992; Shimizu, 1980) and consists of potassium dititanate hydrate, $K_2Ti_2O_5$·xH_2O containing a certain amount of crystal water, $K_{2-x}H_xTi_2O_5$ containing certain protons in interlayers, and $K_2Ti_2O_5$ (Andersson, 1960, 1961; Fujiki, 1988; Masaki, 2000; Uchida, 2001). Potassium dititanate has been the focus of intense research interests because of the interchangeable crystal structure that facilitates subsequent conversions into inorganic–organic/inorganic composites and new layered

Correspondence concerning this article should be addressed to N.-Z. Bao at nzh_bao@yahoo.com.

or three-dimensionally bonded compounds (Clearfield, 1988; Ogawa, 1995; Sasaki, 1994; Schaak, 2002) with special photochemical applications of photoluminescence and photocatalysis (Inoue, 1991; Kudo, 1993, 1997a, 1998; Ogawa, 1995; Schaak, 2002; Yagi, 2001; Yahya, 2001; Yin, 2000). Potassium dititanate ($K_2Ti_2O_5$) exhibits the highest catalytic activity and photoluminescence, even at room temperature, compared to that of other layered titanates (Kudo, 1993, 1997a,b, 1998; Ogawa, 1995; Shibata, 1987; Uchida, 2001; Yin, 2000); from $K_2Ti_2O_5$ many host–guest compounds exhibiting strong blue luminescence and highly improved photochemical activity, even without Pt cocatalysts, have been prepared (Kudo, 1993, 1997a, 1998; Shibata, 1987). These properties and applications have direct relation to morphologies, sizes, water contents, and crystallinities of potassium dititanates (Kudo, 1993, 1997b, 1998; Ogawa, 1995; Shibata, 1987; Yagi, 2001).

Since the first discovery of potassium dititanate (Andersson, 1960), much attention has been given to calcination syntheses of potassium dititanate ($K_2Ti_2O_5$) from crystalline precursors of anatase and rutile at $T > 1000$°C or to ion-exchange syntheses of proton potassium dititanate ($K_{2-x}H_xTi_2O_5$) and hydrous potassium dititanate ($K_2Ti_2O_5{\cdot}xH_2O$) from potassium dititanate (Andersson, 1960, 1961; Clearfield, 1988; Fujiki, 1982, 1988; Kudo, 1993, 1997b, 1998; Ogawa, 1995; Shibata, 1987; Shimizu, 1980; Yagi, 2001). However, systematic studies on modulations of morphologies, sizes, water contents, and crystallinities of potassium dititanate and corresponding reaction conditions are still inadequate. Therefore, it is necessary to study the relationship between synthesis conditions and properties of potassium dititanates to determine effective and optimal conditions and to explore low-cost, large-scale controllable calcination syntheses of pure potassium dititanates with a diversity of morphologies, sizes, water contents, and crystallinities.

The thermodynamic model and calculation were used to estimate the possibility of a reaction, to predict optimum reaction conditions, and to design efficient synthesis routes in material syntheses. For the ion-exchange synthesis, we have established an ion-exchange thermodynamic model to understand the ion-exchange process and determine ion-exchange conditions for optimum syntheses of $K_2Ti_6O_{13}$ and TiO_2 from $K_2Ti_4O_9$ (Bao, 2002c). For hydrothermal syntheses of perovskites, such as $PbTiO_3$, $BaTiO_3$, $SrTiO_3$, $CaTiO_3$, $Pb(Zr,Ti)O_3$, and so on, Riman's research group (Lencka and Riman, 1993a,b, 1995) proposed a thermodynamic model-based approach that makes it possible to predict equilibrium states of hydrothermal reactions on the basis of standard-state data for all possible solid and soluble species. However, further experimental verifications were required in these studies because of some estimated methods and data used in calculations.

In the present study, thermodynamic calculations were used to study the influence of titania reactants on the lowest generation temperature of potassium dititanate by calcination. Because of the lack of comprehensive thermodynamic properties for all compounds, we atempted to obtain the data from handbooks (Karapemjants, 1968; Malcolm, 1998; Stull, 1971) and primary literature (Khakonov, 1974; Lencka 1993b; 1995), or by the estimated method in the primary literature (Criss, 1964) and the regression equation with deviation of $<5\%$. As a result, thermodynamic calculation results are reliable only to a certain extent, and thus we need further experimental verifications. Furthermore, properties and catalytic activities of potassium dititanate have a direct relation to morphologies, sizes, crystallinities, water contents, and the existence state of water, in particular. These have a direct relation to kinetic factors controlling the crystal growth in calcinations and can be determined only by experiments. In this study we used amorphous $TiO_2{\cdot}nH_2O$ as a reactant to directly prepare potassium dititanate with different morphologies, sizes, and crystallinities, and decreasing water contents and changeable existence states by stably increasing the reaction temperature after the potassium dititanate, with the largest water content, is formed at the lowest temperature. These are beneficial for the further controllable industrial production of potassium dititanates.

Thermodynamic Feasibility of Syntheses of Potassium Dititanate from Different Reactants

The Gibbs function is usually used to estimate the direction of a spontaneous change of a chemical reaction, and gives possible reaction conditions such as temperature and pressure after these reaction conditions are quantitatively correlated to the thermodynamic calculation for determining the Gibbs energy of the reaction of the formation of the intended product (Smith, 1975).

For generalized chemical reactions, the Gibbs energy change at constant pressure with the change of temperature is expressed by

$$\Delta G^0_{f,T} = \Delta H^0_{f,298} - T\Delta S^0_{f,298} + \int_{298}^{T} \Delta C_P dT - T\int_{298}^{T} \Delta C_P dT/T \tag{1}$$

where$\Delta G^0_{f,T}$, $\Delta H^0_{f,T}$, and $\Delta S^0_{f,T}$ are changes of Gibbs energy, enthalpy, and entropy, respectively. C_P is heat capacity. If the Gibbs energy change at constant pressure and a certain temperature is ≤ 0, the reaction will have a tendency to roll from left to right.

Reaction equations for preparing potassium dititanate from $TiO_2{\cdot}nH_2O$ and anatase are expressed by Eqs. 2 and 3, respectively.

$$K_2CO_3 + 2TiO_2\ (\text{anatase}) \rightarrow K_2Ti_2O_5 + CO_2 \tag{2}$$

$$K_2CO_3 + 2TiO_2 \cdot nH_2O \rightarrow K_2Ti_2O_5 + CO_2 + 2nH_2O \tag{3}$$

In thermodynamic calculations for $\Delta G^0_{f,T}$ of reactions 2 and 3 with the change of the temperature, we first obtain $\Delta G^0_{f,298}$, $\Delta H^0_{f,298}$, or $S^0_{f,298}$, and the relation between C_P and temperature for all solid compounds, and then use the software packages of Supcrt92, edited by Professor Helgeson (Johnson and Helgeson, 1992), to calculate thermodynamic properties of compounds at arbitrary temperature and pressure. In Eq. 1, for ordinary compounds of CO_2, H_2O, K_2CO_3 and anatase, their $\Delta G^0_{f,298}$, $\Delta H^0_{f,298}$, $S^0_{f,298}$, and the relation between C_P and temperature were obtained form handbooks (Karapemjants, 1968; Malcolm, 1998; Stull, 1971) and Supcrt92 (Johnson and Helgeson, 1992). For $TiO_2{\cdot}nH_2O$, its thermodynamic properties of $\Delta G^0_{f,298}$, $\Delta H^0_{f,298}$, and $S^0_{f,298}$ were obtained from the primary literature (Lencka, 1993b, 1995). However, it is diffi-

Table 1. Standard Thermodynamic Properties of Reactants and Resultants

Material	$\Delta G^0_{f,298}$ (4.2 kJ mol^{-1})	$\Delta H^0_{f,298}$ (4.2 kJ mol^{-1})	$S^0_{f,298}$ (4.2 J mol^{-1} K^{-1})	$C_P = C_1 + C_2T + C_3/T^2$ (4.2 J mol^{-1} K^{-1})		
				C_1	10^3C_2	$10^{-5}C_3$
$TiO_2 \cdot nH_2O$	−255.06[a]	−282.04[a]	22.2116[a]	22.1191[b]	0	0.24984[b]
Anatase[c]	−204.86	−218.1	11.93	17.83	0.5	−4.23
$K_2Ti_2O_5$	−540.831[d]	−597.627[e]	−22.412[d]	93.6012[b]	8.65[b]	2.08814[b]
K_2CO_3[e]	−248.773	−274.900	37.170	23.405	22.0	−2.368
CO_2[e]	−94.254	−94.051	51.085	10.570	2.16	−2.06
H_2O[e]	−54.525	−57.935	44.763	12.665	−10.40	0.0131

Sources: a: Lencka (1993b, 1995); b: Criss (1964); c: Karapemjants (1968); d: Calculated from Eqs. 4 and 5; e: Khakonov (1974); f: Johnson et al. (1992).

cult to obtain all of thermodynamic properties of some compounds that have only one thermodynamic property; for example, we can obtain only $\Delta H^0_{f,298}$ of $K_2Ti_2O_5$ from the primary literature (Khakonov, 1974). Thus other thermodynamic properties of $K_2Ti_2O_5$ were obtained by the regression of thermodynamic data of several thousands of solid compounds in handbooks of thermodynamic properties of compounds. The simplified equation for estimating $\Delta G^0_{f,298}$ and $\Delta H^0_{f,298}$ of $K_2Ti_2O_5$ is given by

$$\Delta G^0_{f,298} = (\Delta H^0_{f,298} + 12822.8)/1.10501 \text{ J/kmol} \quad (4)$$

The deviation of Eq. 4 is <5%. Combined with the following precise equation, we obtain $\Delta G^0_{f,298}$ and $S^0_{f,298}$ for $K_2Ti_2O_5$:

$$\Delta G^0_{f,298} = \Delta H^0_{f,298} - 298\Delta S^0_{f,298} \quad (5)$$

The relations between C_P and temperature for both $TiO_2{\cdot}nH_2O$ and $K_2Ti_2O_5$ are estimated by the Criss–Coble method (Criss, 1964).

The above standard thermodynamic properties of reactants and products in our calculations for reaction Eqs. 2 and 3 are summarized in Table 1. The free energy for reactions of anatase and $TiO_2{\cdot}nH_2O$ with K_2CO_3 to generate potassium dititanate at 25–1200°C was estimated as shown in Figure 1. It can be found that the Gibbs free energy changes are lower than zero at $T > 508$°C for the reaction Eq. 1 and at $T > 295$°C for the reaction Eq. 2, respectively, indicating that estimated starting generation temperatures for preparing potassium dititanate from anatase and $TiO_2{\cdot}nH_2O$ are 508 and 295°C, respectively. These estimated temperatures are far lower than the reported temperature of 1000°C (Andersson, 1960, 1961; Fujiki, 1982, 1988; Kudo, 1993, 1997b, 1998; Ogawa, 1995; Shibata, 1987; Shimizu, 1980; Yagi, 2001).

Because of the lack of comprehensive thermodynamic properties for all compounds, we attempted to obtain precise data from handbooks, primary literature, or by some estimated methods in the primary literature and the regression method with deviation of <5%. Thermodynamic calculation results confirmed that amorphous $TiO_2{\cdot}nH_2O$ can decrease the lowest generation temperature of potassium dititanate because of its high reaction activity compared to that of anatase. This agrees with similar thermodynamic calculations for hydrothermal syntheses of some perovskites (Lencka, 1993a,b, 1995). However, further experimental verifications are still required for obtaining precise results (Bao, 2002c; Lencka, 1993a, 1993b, 1995). Properties and catalytic activities of potassium dititanate have direct relations to morphologies, sizes, crystallinities, and water contents and corresponding existence states of water, in particular. Potassium dititanate containing water with different contents and states usually cannot be prepared directly from anatase. Efficient synthesis temperatures and products of potassium dititanates with a diversity of morphologies, sizes, water contents, and crystallinities were determined by further experiments.

Experimental

Sample preparation

The starting materials, $TiOSO_4$, TiO_2 (anatase), and K_2CO_3, were commercially available with purities of 99.5%. $TiO_2{\cdot}nH_2O$ (hydrous titanium dioxide) was prepared by hydrolyzing $TiOSO_4$ in hot water with vigorous stirring. Deionized water was added to both the mixture of anatase and K_2CO_3 and the mixture of $TiO_2{\cdot}nH_2O$ and K_2CO_3. The chemical compositions (TiO_2/K_2O molar ratio) were controlled at 2.05. The

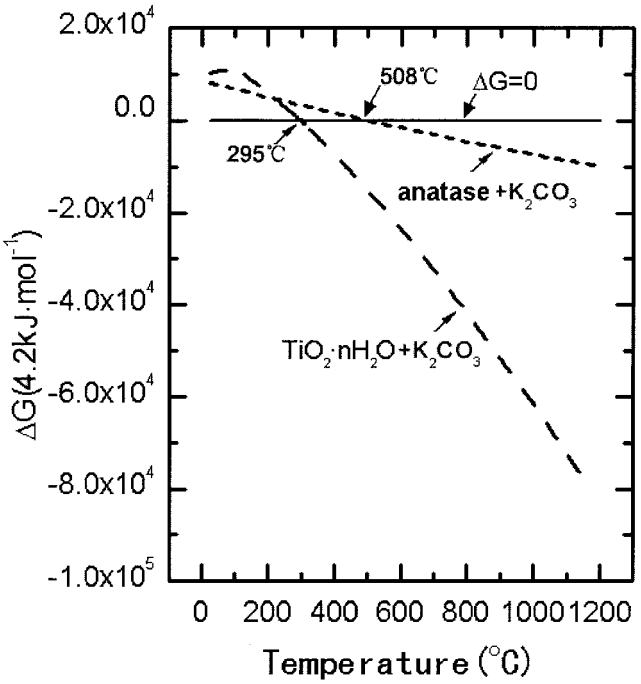

Figure 1. The Gibbs free energy changes for reactions of anatase and $TiO_2{\cdot}nH_2O$ with K_2CO_3 to form $K_2Ti_2O_5$, calculated by Supcrt92.

mixture processes were preformed by ball milling with water. Final mixtures were dried in an oven at 90°C for 10 h.

Calcinations were performed in a muffle furnace at a heating rate of 10°C/min, using the heating instrument (Model AI-708, Xiameng Yuguang Electronic Technology Institute, Xiamen, China). Samples designated A1–A10 were obtained by sintering dried reactant mixtures of anatase and K_2CO_3 at 350, 400, 500, 600, 650, 700, 750, 800, 850, and 900°C, respectively, for 2 h. Samples designated B0–B10 were obtained by sintering dried reactant mixtures of $TiO_2{\cdot}nH_2O$ and K_2CO_3 at 300, 350, 400, 500, 600, 650, 700, 750, 800, 850, and 900°C, respectively, for 2 h. All samples were removed from the furnace at corresponding calcination temperatures and cooled in air. All samples were leached in water at 90°C for 2 h to dissolve hydrosoluble and noncrystalline components for obtaining crystal components in samples.

Characterizations

Thermogravimetric analysis–differential thermal analysis (TGA-DTA, Model SDT 2960, TA Instruments, New Castle, DE) was performed on the dried reactant mixtures of (a) the anatase–K_2CO_3 mixture and (b) the $TiO_2{\cdot}nH_2O$–K_2CO_3 mixture, both with the TiO_2/K_2O molar ratio of 2.05 at the heating rate of 20°C/min up to 1200°C in flowing nitrogen gas. Data acquisition was performed on-line, and the data were exported as images. X-ray powder diffraction patterns were obtained using a D8 advance (Bruker AXS, Karlsruhe, Germany). Cu–K_α radiation with a nickel filter and a zero-background sample cell were used, operating at 40 kV and 20 mA. All samples were measured in the continuous scan mode at 5–80° (2θ) with a scanning rate of 0.02° (2θ)/s. Peak positions and relative intensities of crystal products were characterized by comparing to JCPDS (the Joint Committee for Powder Diffraction Standards) files. Morphologies of crystalline components in all samples were observed by optical microscope (Model Galen III, Jiangnan Optical Instrument Co., Ltd., Nanjing, China). A representative potassium dititanate, prepared from $TiO_2{\cdot}nH_2O$, was observed by high-resolution transmission electron microscopy (HRTEM, JEM2010, JEOL, Tokyo, Japan). UV–visible diffuse reflectance spectra were recorded on a Jasco V-500 spectrophotometer (Jasco, Tokyo, Japan), equipped with an integrating sphere. Powder samples were loaded in a quartz cell and the measurement was taken in a wavelength range of 200–800 nm against a standard.

Results and Discussion

Reaction process and phase transformations

TGA-DTA traces of the anatase–K_2CO_3 mixture and the $TiO_2{\cdot}nH_2O$–K_2CO_3 mixture, both with a TiO_2/K_2O molar value of 2.05, are shown in Figure 2a and b, respectively, illustrating that the reaction process occurred in calcinations.

The TGA trace for the anatase–K_2CO_3 mixture exhibits two obvious weight-loss steps (see Figure 2a). A first weight loss step, attributed to the rapid decrease of free water, occurs at 100–220°C and corresponds to an obvious endothermic peak at 180°C. The TGA trace after the first weight-loss step is horizontal at 220–500°C, and no endothermic peak is observed on the DTA trace at 220–500°C, which indicates that no reaction occurred between anatase and K_2CO_3 at $T < 500$°C. A second

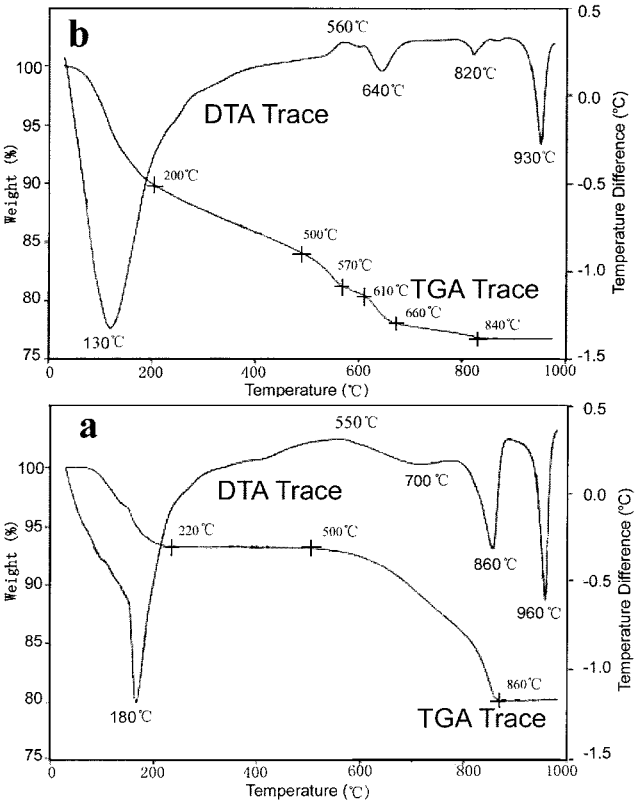

Figure 2. TGA-DTA traces of (a) the mixture of anatase and K_2CO_3 and (b) the mixture of $TiO_2{\cdot}nH_2O$ and K_2CO_3, both with the same TiO_2/K_2O molar ratio of 2.05.

weight-loss step is observed at a higher temperature ranging from 500 to 860°C, corresponding to a very broad exothermic peak centered at 550°C, a very broad endothermic peak centered around 700°C, and an endothermic peak at 860°C, on the DTA trace. About 15% weight loss at 500–860°C agrees with the theoretical release of CO_2 through the decomposition of K_2CO_3 contained in the powder mixture. In addition, the reaction between titanium and potassium oxide occurs simultaneously at 500–860°C, ending with a final crystallization reaction, indicated by the endothermic peak at 860°C on the DTA trace, of $K_2Ti_2O_5$. No weight-loss step is observed at $T >$ 860°C. One endothermic peak, attributed to the phase change from $K_2Ti_2O_5$ to $K_2Ti_4O_9$, appears on the DTA trace at 960°C, agreeing with our previous results (Bao, 2002a). With respect to the second weight loss, its starting temperature of 500°C agrees with 508°C calculated by the thermodynamic calculation.

In Figure 2b, a continue weight-loss line with various slopes is observed at 100–840°C on the TGA trace. The starting weight loss at $T < 200$°C is attributed to the rapid decrease of the free water, corresponding to a broad endothermic peak centered at 130°C on the DTA trace. The following weight loss at 200–500°C is relatively slow and steady. The weight loss then accelerates at 500–570 and 610–660°C and corresponds to a small broad exothermic peak centered at 560°C and an endothermic peak at 640°C, respectively, on the DTA trace. The weight loss at 500–660°C is less than the theoretical

weight loss attributed to the decomposition of K_2CO_3 of the powder mixture, so that we believe that the weight loss at 200–500°C is attributed to both the dehydration of $TiO_2{\cdot}nH_2O$ and the slow decomposition of K_2CO_3 that result in the slow reaction between titanium and potassium oxides to form potassium dititanate hydrate. On the DTA trace, the weak and broad exothermic peak centered at 560°C and the endothermic peak at 640°C are attributed to the dehydration of the potassium dititanate hydrate and the crystallization of potassium dititanate containing certain crystalline water, respectively. The final weight loss at 660–840°C is attributed to the dehydration of potassium dititanate containing certain crystalline water, ending with the generation of the $K_2Ti_2O_5$ at 820°C. After calculating the weight loss at 660–840°C, we obtain the chemical formula of $K_2Ti_2O_5{\cdot}0.35H_2O$ generated from the potassium dititanate hydrate at 640°C. The continuous weight loss at 200–840°C indicates that the decomposition of K_2CO_3, the dehydration of $TiO_2{\cdot}nH_2O$, and the reaction between titanium and potassium oxide occur simultaneously at 200–840°C. No weight-loss step is observed at $T > 840$°C. One endothermic peak attributed to the phase change from $K_2Ti_2O_5$ to $K_2Ti_4O_9$ appears on the DTA trace at 940°C.

To accurately identify phase types and some detailed information about crystal growths of crystal components generated at various temperatures, we designed experiments and prepared a serials of representative samples designated A1–A10 for the anatase–K_2CO_3 system and designated B0–B10 for the amorphous $TiO_2{\cdot}nH_2O$–K_2CO_3 system, according to the thermodynamic calculation results and the TGA-DTA results. Phase identifications for all samples were conducted using the XRD patterns shown in Figure 3 and Figure 4. Diffraction peaks for all samples were indexed with respect to corresponding components in the JCPDS files.

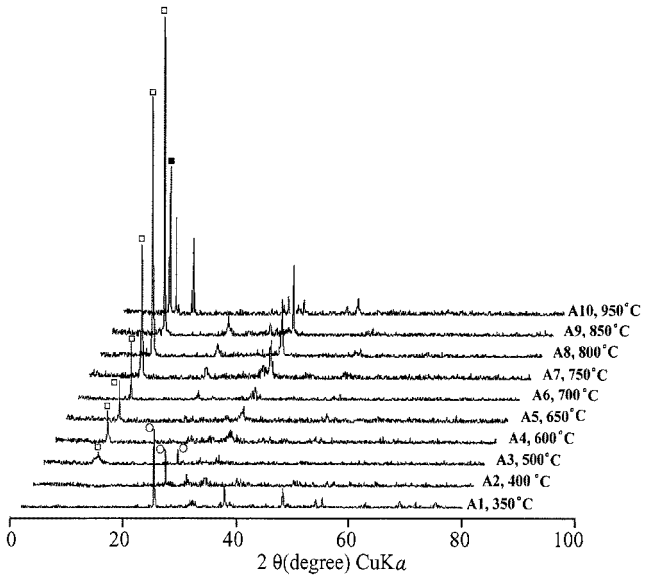

Figure 3. X-ray powder diffraction patterns of samples A1–A10 prepared by sintering the dried anatase–K_2CO_3 mixture at 350, 400, 500, 600, 650, 700, 750, 800, 850, and 950°C, respectively, for 2 h.

The strongest characteristic peaks of crystalline components are marked with □ ($K_2Ti_2O_5$), ■ ($K_2Ti_4O_9$), and ○ (anatase).

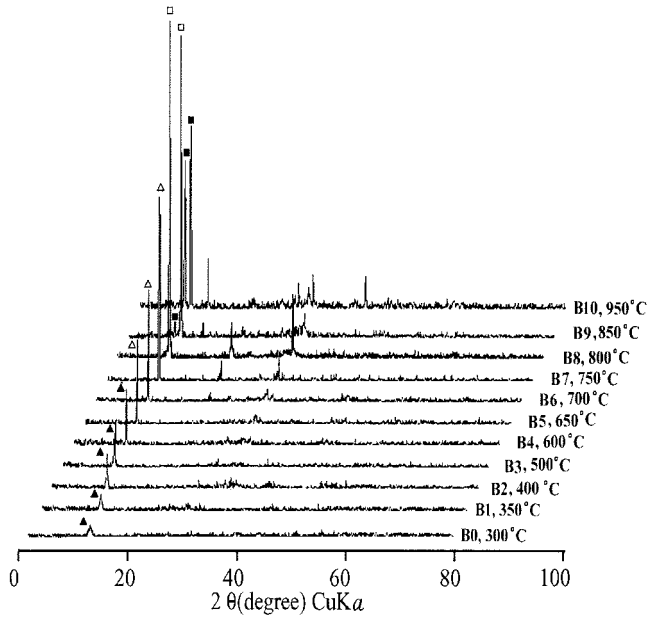

Figure 4. X-ray powder diffraction patterns of samples B0–B10 prepared by sintering the dried $TiO_2{\cdot}nH_2O$–K_2CO_3 mixture at 300, 350, 400, 500, 600, 650, 700, 750, 800, 850, and 950°C, respectively, for 2 h.

The strongest characteristic peaks of crystalline components are marked with ▲ (potassium dititanate hydrates), △ ($K_2Ti_2O_5{\cdot}0.35H_2O$), □ ($K_2Ti_2O_5$), and ■ ($K_2Ti_4O_9$).

In Figure 3, both A1 and A2 are anatase. A3 is mostly anatase with a certain amount of $K_2Ti_2O_5$ (JCPDS card No. 13-448). The broadening of the strongest XRD characteristic peak of $K_2Ti_2O_5$ in A3 indicates the formation of $K_2Ti_2O_5$ nanoclusters at 500°C, agreeing with both the 508°C obtained by our thermodynamic calculation results and the TGA-DTA results. A4–A9 are all $K_2Ti_2O_5$. The width of the strongest characteristic peak of $K_2Ti_2O_5$ from A3 to A9 become narrower, indicating a crystal growth of $K_2Ti_2O_5$ with increase of reaction temperature. Meanwhile, the increasing peak intensity for the same peak of $K_2Ti_2O_5$ from A3 to A9 also indicates an increasing crystallinity of $K_2Ti_2O_5$ with increasing reaction temperature. We can also observe that the peak intensity of $K_2Ti_2O_5$ obviously increases from A7 to A9, which is attributed to the accelerated formation of $K_2Ti_2O_5$ at 700–860°C. This agrees with a very broad endothermic peak centered at 700°C and corresponding rapid weight loss on the TGA-DTA traces of Figure 2b. A10 is a typical XRD pattern of $K_2Ti_4O_9$ (JCPDS card No. 27-447).

In Figure 4, the positions of the strongest peak for XRD patterns of B0–B8 are all well indexed to the strongest characteristic peak of potassium dititanate (JCPDS card No. 13-448). Combined with the TGA-DAT results, products for B0–B4, B5–B7, and B8 are potassium dititanate hydrate, $K_2Ti_2O_5{\cdot}0.35H_2O$, and $K_2Ti_2O_5$, respectively. B9 is mostly $K_2Ti_2O_5$ with a certain amount of $K_2Ti_4O_9$ (JCPDS card No. 27-447). B10 is pure potassium tetratitanate. The width of the strongest peak from B0 to B9 becomes narrower, indicating a crystal growth of potassium dititanate with increasing reaction temperature. Meanwhile, the peak intensity for the same peak

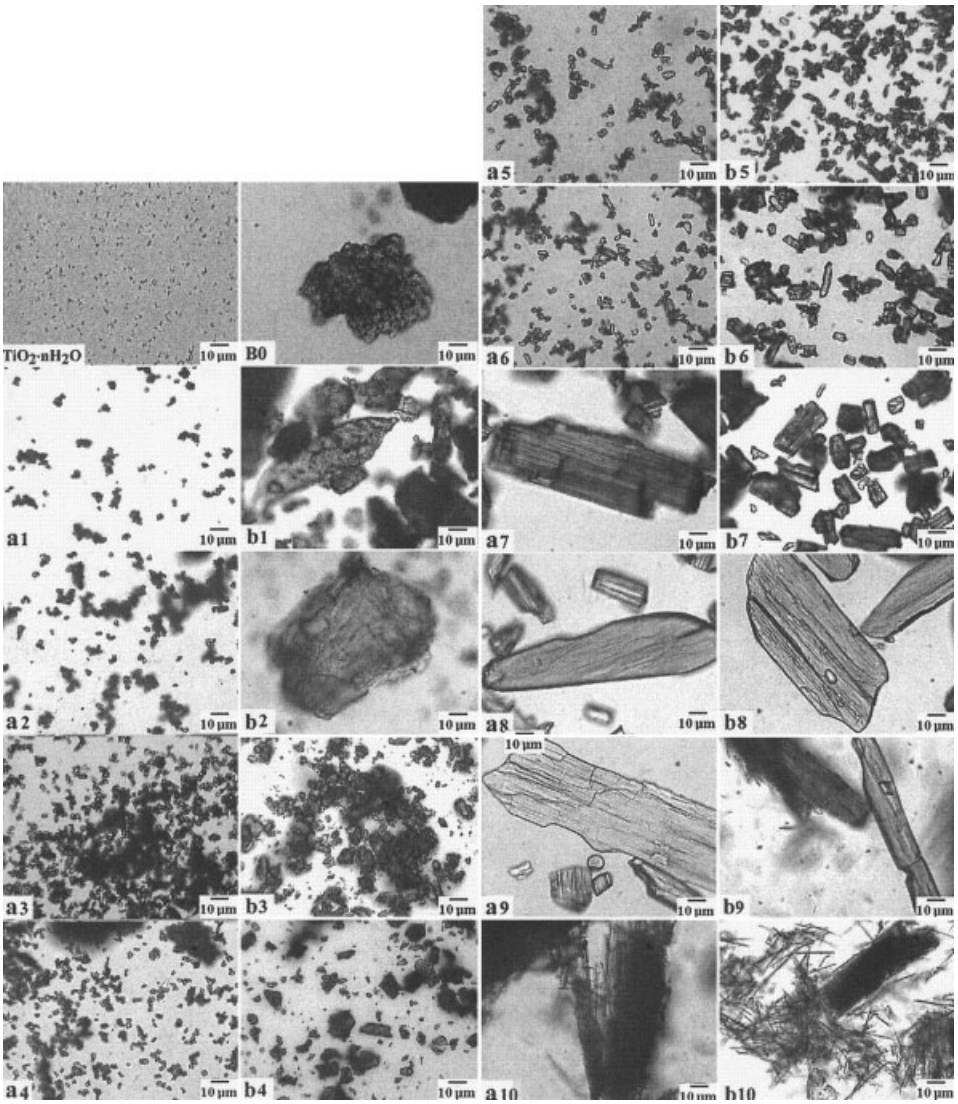

Figure 5. Optical micrographs of crystalline components.

Figures a1–a10 show, respectively, optical micrographs of crystalline components in samples A1–A10 prepared by sintering the dried anatase–K_2CO_3 mixture at 350, 400, 500, 600, 650, 700, 750, 800, 850, and 950°C, respectively, for 2 h. Figures b0–b10 show optical micrographs of crystalline components in samples B0–B10 prepared by sintering the dried $TiO_2{\cdot}nH_2O$–K_2CO_3 mixture at 300, 350, 400, 500, 600, 650, 700, 750, 800, 850, and 950°C, respectively, for 2 h. Figure $TiO_2{\cdot}nH_2O$ shows the optical micrograph of the hydrous $TiO_2{\cdot}nH_2O$. All samples were dispersed in water at 90°C to dissolve the hydrosoluble and noncrystalline components. Scale bars for all samples are 10 μm.

from B0 to B9 becomes stronger, indicating an increasing crystallinity of potassium dititanate with increasing reaction temperature. Further, the formation of potassium dititanate hydrate in the B0 sample at 300°C agrees with the 295°C obtained by our thermodynamic calculation. Because of the increasing crystallinity for $K_2Ti_2O_5$ generated from $K_2Ti_2O_5{\cdot}0.35H_2O$ by the dehydration reaction, the number of characteristic peaks of potassium dititanate increases from B5.

As a result, replacing anatase with amorphous $TiO_2{\cdot}nH_2O$ in reactant mixtures will change the reaction process and the lowest generation temperatures for the target potassium dititanates.

Morphologic evolution

All samples were dispersed respectively in water at 90°C for dissolving the hydrosoluble and noncrystalline components, as well as the K_2CO_3 reactant and the K_2O-rich hydrosoluble and noncrystalline melt generated. Crystal components in all samples were then observed by optical microscope.

Optical micrographs of Figure 5a1–a10 show morphologies and sizes of crystal components in samples A1–A10 prepared by sintering the dried anatase–K_2CO_3 mixture at 350, 400, 500, 600, 650, 700, 750, 800, 850, and 950°C, respectively, for 2 h, indicating the crystal growth for potassium dititanates prepared from anatase. Optical micrographs of Figure 5b0–b10 show morphologies and sizes of crystal components in samples B0–B10, prepared by sintering the dried $TiO_2{\cdot}nH_2O$–K_2CO_3 mixture at 300, 350, 400, 500, 600, 650, 700, 750, 800, 850, and 950°C, respectively, for 2 h, indicating the crystal growth for potassium dititanates prepared from $TiO_2{\cdot}nH_2O$. The optical micrograph of $TiO_2{\cdot}nH_2O$ in Figure 5 shows the morphology and size of the hydrous $TiO_2{\cdot}nH_2O$.

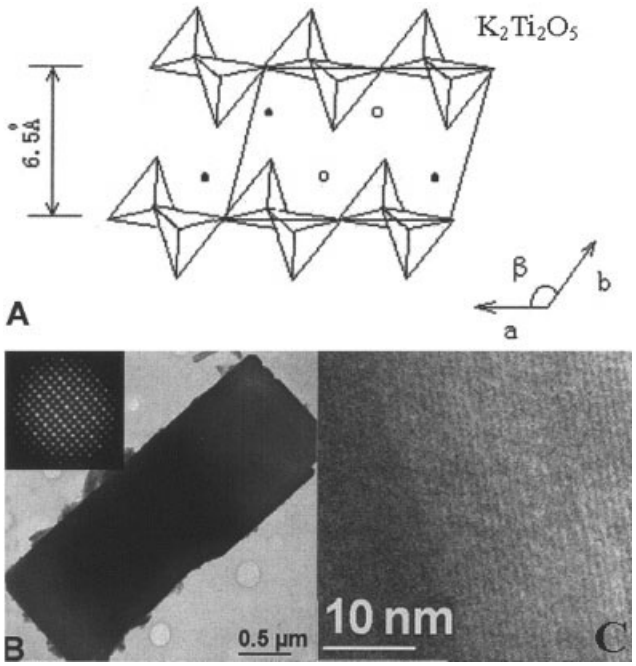

Figure 6. (A) Idealized crystal structure of $K_2Ti_2O_5$ with a layered structure.

The Ti atom in $K_2Ti_2O_5$ is bonded to five oxygens that are grouped in the form of a trigonal bipyramid, somewhat distorted. The infinite two-dimensional sheets in direction of c and a consist of the composition $(Ti_2O_5)^{2-}$. Sheets are then separated from one another by the K^+ ions, each having eight oxygens as neighbors. (B) TEM image and electron diffraction pattern (the inset) of a perfect $K_2Ti_2O_5$ single crystal. (C) High-resolution TEM image of an individual $K_2Ti_2O_5$ single crystal.

Particles in Figure 5a1–a2 are all anatase, determined by XRD analysis, whereas particles in Figure 5a3 are anatase containing a little $K_2Ti_2O_5$. The reaction between K_2CO_3 and anatase occurs at $T < 500$°C. Because of both the initial stage of reaction between anatase and K_2CO_3 and the formation of very fine $K_2Ti_2O_5$ particles indicated by the very broad characteristic peak of $K_2Ti_2O_5$ in the XRD pattern of Figure 4A3, particles in Figure 5a1–a3 have the same morphology and size, and mainly consist of the anatase reactant. Figure 5a3 and Figure 5a4 show smaller spherelike particles and rodlike irregular particles, respectively. Particle sizes become larger from Figure 5a3 to Figure 5a6, in turn, and particles in Figure 5a4–a6 are rodlike in appearance. These indicate a continuous crystal growth for $K_2Ti_2O_5$ with increasing reaction temperature from 500 to 700°C, in agreement with both the starting reaction temperature of 508°C obtained by our thermodynamic calculation and a weight loss starting from 500°C on the TGA trace of Figure 2a. Because of the accelerated crystallization reaction for $K_2Ti_2O_5$ at 700–860°C, an abrupt morphologic change is observed from Figure 5a6 to Figure 5a7. Crystals in Figure 5a7, Figure 5a8, and Figure 5a9, respectively, are radially aligned columnlike rods, large single crystals, and much larger single crystals, indicating a continuous crystal growth at 700–860°C. These agree with the increasing peak number and peak intensity in XRD patterns of Figure 3A6–A7, a very broad endothermic peak centered at 700°C, and corresponding rapid weight loss at 700–860°C on the TGA-DTA traces of Figure 2a. Because of increasing crystallinities and sizes, crystals in Figure 5a7–a9 become brighter under visible light. A10 is $K_2Ti_4O_9$ whiskers.

Figure 5$TiO_2{\cdot}nH_2O$ shows that the amorphous $TiO_2{\cdot}nH_2O$ reactant is fine particles, whereas B0 is bulk potassium dititanate hydrates (see Figure 5b0) determined by XRD analysis (see Figure 4B0). This indicates that the reaction between $TiO_2{\cdot}nH_2O$ and K_2CO_3 occurs at 300°C, agreeing with the starting reaction temperature of 295°C obtained by our thermodynamic calculation. B0 and B2 are bulks coated by some amorphous $TiO_2{\cdot}nH_2O$ fine particles (see Figure 5b0–b2), whereas a relatively clean surface is observed for bulks of B2 (see Figure 5b2). XRD analysis shows that the characteristic peak of potassium dititanate hydrates from B0 to B2 becomes narrower and stronger (see Figure 4B0–B2), indicating a crystal growth of potassium dititanate hydrates attributed to the continuous reaction between $TiO_2{\cdot}nH_2O$ and K_2CO_3. A morphologic comparison between B2 (see Figure 5b2) and B3–B5 (see Figure 5b3–b5) shows that B3 is formed from bulk crys-

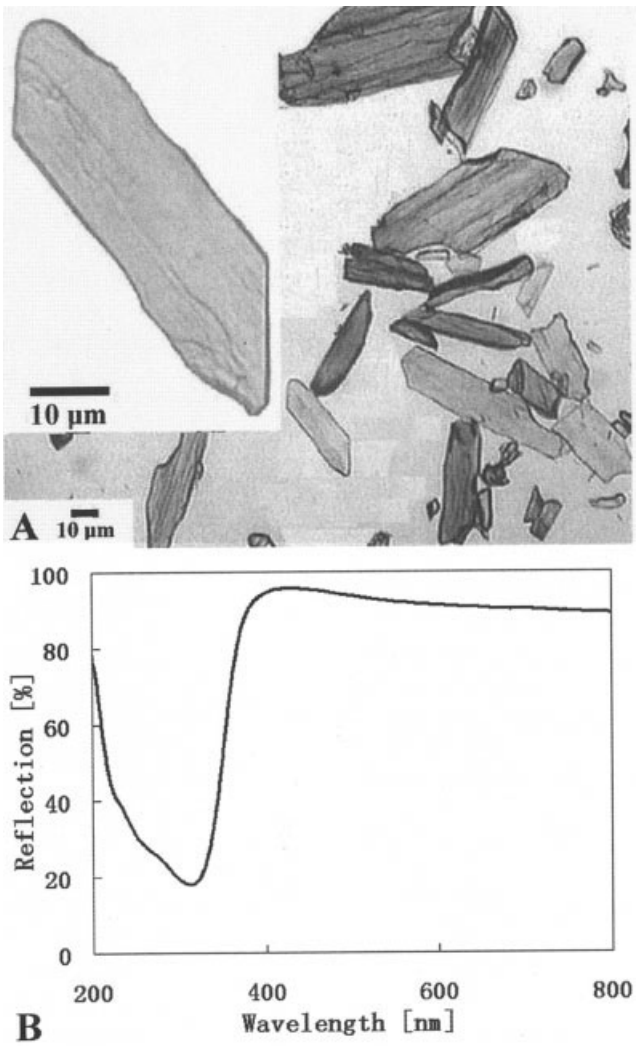

Figure 7. Optical micrograph (A) and UV–visible diffuse reflectance spectra (B) for potassium dititanate prepared from $TiO_2{\cdot}nH_2O$ by calcination at 800°C.

The insert in A shows a magnified optical micrograph of a perfect $K_2Ti_2O_5$ single crystal. The scale bars both indicate 10 μm.

Table 2. Summarized Synthesis Temperatures and Characteristics of Products (Potassium Dititanates) Prepared from Amorphous $TiO_2 \cdot nH_2O$ and Anatase

Precursor	Reaction Tempeature °C	Chemical Component	Intensity, Width (Shape), and Number*	Morphology of Crystals	Size (Average Diameter)** (μm)
$TiO_2 \cdot nH_2O$	<300	$TiO_2 \cdot nH_2O$	no	spherelike, fine	$<1 \times 1$, (<1.1)
	300	$K_2Ti_2O_5$ hydrate	weakest, narrow, 1	bulk,	50×50, (56)
	350	$K_2Ti_2O_5$ hydrate	weaker, broadest, 1	bulk,	$>30 \times 30$, (>34)
	400	$K_2Ti_2O_5$ hydrate	weak, broad, 1	bulk	65×80, (81)
	500	$K_2Ti_2O_5$ hydrate	strong, sharp, 1	irregular	10×10, (11.3)
	600	$K_2Ti_2O_5$ hydrate	strong, sharp, 1	irregular	9×9, (10.2)
	650	$K_2Ti_2O_5 \cdot 0.35H_2O$	stronger, sharper, 3	short rod, irregular	4×8, (6.4)
	700	$K_2Ti_2O_5 \cdot 0.35H_2O$	stronger, sharper, 3	rod	5×16, (6.4)
	750	$K_2Ti_2O_5 \cdot 0.35H_2O$	stronger, sharper, 3	radially aligned columnlike rods	6×25, (10.1)
	800	$K_2Ti_2O_5$	strongest, sharpest, 3	flat platelike single crystal	35×120, (73)
	850	$K_2Ti_2O_5$, $K_2Ti_4O_9$	stronger, sharper, 3	column	16×110, (47)
	950	$K_2Ti_4O_9$	no	whisker	0.3×30, (3.4)
Anatase	350	anatase	no	spherelike	1.5, (1.7)
	400	anatase	no	spherelike	1.5, (1.7)
	500	anatase, $K_2Ti_2O_5$	weaker, broadest, 1	spherelike	1.5, (1.7)
	600	$K_2Ti_2O_5$	weak, broad, 1	spherelike	3.5, (4)
	650	$K_2Ti_2O_5$	strong, sharp, 2	short rod, spherelike	3×8, (3–5)
	700	$K_2Ti_2O_5$	strong, sharp, 3	rod,	3×10, (4–6)
	750	$K_2Ti_2O_5$	stronger, sharper, 3	radially aligned columnlike rods	40×120, (78)
	800	$K_2Ti_2O_5$	stronger, sharper, 3	flat platelike	30×140, (73)
	850	$K_2Ti_2O_5$	strongest, sharpest, 3	flat platelike single crystal	40×140, (84)
	950	$K_2Ti_4O_9$	no	whisker	1.3×100, (13)

* Intensity, width (shape), and number of characteristic peaks of potassium dititanates shown in XRD patterns of Figure 3 and Figure 4.
**The size of crystals is obtained by measuring the size of projected images in optical micrographs. Average diameter is the equivalent projected area diameter calculated by $\sqrt{(4 \times S_a)/\pi}$, where S_a is the projected area of particles in micrographs.

tals of B2 and B3–B5 are relatively smaller crystals. Increasing peak intensities from B2 to B5 (see Figure 4B2–B5), an accelerated weight loss at 500–660°C (see the TGA trace in Figure 2b), and corresponding broad exothermic peak centered at 560°C (see the DTA trace in Figure 2b) indicate that the morphologic evolution from B2 to B5 is attributed to the dehydration and the crystallization of potassium dititanate hydrates that finally convert into $K_2Ti_2O_5 \cdot 0.35H_2O$ crystals (see Figure 5b5) at 650°C. Figure 5b5–b8 show that B5 is small rods; B6 is large rods; B7 is radially aligned columnlike rods; and B8 is bulk single crystals, indicating the continuous crystal growth and the morphologic evolution from B5 to B8. In addition, the increasing crystallinities from B5 to B8 were observed in corresponding XRD patterns (see Figure 4B5–B8), and the weight loss and corresponding endothermic peak at 650–800°C are also observed on the TGA-DTA traces in Figure 2b. These indicate that the continuous crystal growth and the morphologic evolution from B5 to B8 are attributed to the dehydration of $K_2Ti_2O_5 \cdot 0.35H_2O$ and the crystallization reaction of $K_2Ti_2O_5$. The morphologic comparison between B8 (see Figure 5b8) and B9 (see Figure 5b9) shows that B9 is mostly $K_2Ti_2O_5$ single crystals with defects and relatively smaller crystal size. This is attributed to the generation of a little $K_2Ti_4O_9$ whiskers in B9, known from corresponding XRD pattern (see Figure 4B9). Figure 5b10 shows that B10 is $K_2Ti_4O_9$ whiskers.

Microstructure and optical property of $K_2Ti_2O_5$ single crystal

Figure 6A shows an idealized crystal structure of layered potassium dititanate (Andersson, 1960, 1961). The Ti atoms in $K_2Ti_2O_5$ are bonded to five oxygens that are grouped in the form of a trigonal bipyramid, somewhat distorted. The infinite two-dimensional sheets in direction of c and a are composed of the composition $(Ti_2O_5)^{2-}$ sheets that are then separated from one another by the K^+ ions, each having eight oxygens as neighbors. Figure 6B shows the transmission electron microscope image of a perfected representative $K_2Ti_2O_5$ single crystal, prepared from $TiO_2 \cdot nH_2O$ at 800°C, with a length about 1.5 μm and a width about 3 μm. The insert shows an electron diffraction pattern that was recorded by directing the electron beam onto this single crystal. The electron diffraction pattern could be readily indexed according to the crystal structure (see Figure 6A). A high-resolution transmission electron microscopic image (see Figure 6C) of an individual $K_2Ti_2O_5$ single crystal shows that the spacing of 6.82 $\pm$ 0.33 Å between adjacent lattice planes corresponds to the distance between adjacent $(Ti_2O_5)^{2-}$ sheets, agreeing with the layer distance of 6.3 Å of Figure 6A.

The $K_2Ti_2O_5$ single crystals, synthesized without the size limitation, are observed in the form of optical microscope images in Figure 7A. The insert shows an optical microscope image of a crystal imaged at a higher magnification. The crystals in image are bright, indicating that the $K_2Ti_2O_5$ single crystal reflects most visible light. The UV–visible diffuse reflectance spectrum of $K_2Ti_2O_5$ is depicted in Figure 7B. The spectrum shows an absorption edge of 315 nm that is consistent with the band gap of 3.94 eV. The main absorption range is 210–350 nm and corresponds to >50% absorption of the incoming light with the wavelength < 350 nm. It is also found that there is little absorption (<10%) for incoming light with the wavelength > 390 nm. As a result, potassium dititanate single crystals are bright in Figure 5a6–a9 and b5–b8. Potassium dititanates under visible light becomes brighter form B5 to B8 and from A6 to A9 in Figure 5, which indicates that the

scattering of light increases with increasing the grain size of the potassium dititanate powders.

Low-temperature optimum controllable syntheses of potassium dititanate

Table 2 summarizes potassium dititanates with various morphologies, sizes, crystallinities, and water contents prepared from both anatase and amorphous $TiO_2 \cdot nH_2O$ at 300–850°C. Only $K_2Ti_2O_5$ was prepared from anatase at 500–800°C, whereas when using amorphous $TiO_2 \cdot nH_2O$ as reactant, potassium dititanate hydrates, $K_2Ti_2O_5 \cdot 0.35H_2O$, and $K_2Ti_2O_5$ were synthesized at 300–500, 500–700, and 700–850°C, respectively. The thermodynamic calculation results of 295°C for $TiO_2 \cdot nH_2O$ and 508°C for anatase agree with the designed experimental results of 300°C for $TiO_2 \cdot nH_2O$ and 500°C for anatase, respectively, in calcination syntheses of potassium dititanates. The amorphous $TiO_2 \cdot nH_2O$ lowers the starting generation temperature of potassium dititanates. Even if anatase is used as the reactant, the synthesis temperature of $K_2Ti_2O_5$ is far lower than the temperatures reported in previous studies (Andersson, 1960, 1961; Fujiki, 1982, 1988; Kudo, 1993, 1997b, 1998; Ogawa, 1995; Shibata, 1987; Shimizu, 1980; Yagi, 2001). Properties of potassium dititanates can be tailored by varying their morphologies, sizes, water contents, and crystallinities, which can be achieved by adjusting reactant types and corresponding synthesis conditions.

Conclusions

Thermodynamic calculations coupled with the experimental verifications allowed us to accurately determine the lowest starting reaction temperatures of two kinds of reactant systems of anatase–K_2CO_3 and $TiO_2 \cdot nH_2O$–K_2CO_3 for preparing potassium dititanates in calcination. The thermodynamic calculation results show that phase types and crystallinities of TiO_2 precursors and reaction temperatures are key thermodynamic variables; and that the amorphous $TiO_2 \cdot nH_2O$, with reaction activity higher than that of anatase, can decrease the lowest generation temperature of potassium dititanate. More precise reaction temperatures and crystal growth process were determined by designed experiments. Pure potassium dititanates with various morphologies, sizes, water contents, and crystallinities were prepared under control.

Acknowledgments

The authors appreciate the Outstanding Youth Fund of National Natural Science Foundation (29925616), National High-tech Research Development Program (863 Program: 2003AA333010), and Natural Science Foundation (20246002, 20236010) of China, and the help and facilities of Research Laboratory of Hydrothermal Chemistry, Kochi University, Japan.

Literature Cited

Andersson, S., and A. D. Woadsley, "Five-Coordinated Titanium in $K_2Ti_2O_5$," *Nature*, **187**, 499 (1960).

Andersson, S., and A. D. Wodsley, "Crystal Structure of $K_2Ti_2O_5$," *Acta Chem. Scand.*, **15**, 663 (1961).

Bao, N., X. Feng, X. Lu, and Z. Yang, "Study on the Formation and Growth of Potassium Titanate Whiskers," *J. Mater. Sci.*, **37**(14), 3035 (2002a).

Bao, N., X. Feng, L. Shen, and X. Lu, "Calcination Syntheses of a Series of Potassium Titanates and Their Morphologic Evolution," *Crystal Growth & Design*, **5**, 437 (2002b).

Bao, N., X. Lu, X. Ji, X. Feng, and J. Xie, "Thermodynamic Modeling and Experimental Verification for Ion-Exchange Synthesis of $K_2O \cdot 6TiO_2$ and TiO_2 Fibers from $K_2O \cdot 4TiO_2$," *Fluid Phase Equilib.*, **193**, 229 (2002c).

Chase, Malcolm W., Jr., "NIST-JANAF, Thermochemical Tables," *J. Phys. Chem. Ref. Data*, Monograph 9, 4th Edition (1998).

Clearfield, A., "Role of Ion Exchange in Solid-State Chemistry," *Chem. Rev.*, **88**, 125 (1988).

Criss, C. M., and J. W. Cobble, "The Thermodynamic Properties of High Temperature Aqueous Solutions. V. The Calculation of Ionic Heat Capacities up to 200°, Entropies and Heat Capacities above 200°," *J. Am. Chem. Soc.*, **86**, 5385 (1964).

Feng, X., J. Lü, X. Lu, N. Bao, and D. Chen, "Applications of Potassium Titanate Whiskers in Composite Materials," *Acta Mater. Comp. Sinica*, **16**, 1 (1999).

Fujiki, Y., and T. Mitsuhashi, "Preparation of Potassium Hextitanate Fiber and Its Related Composite Fiber Using Natural Rutile or Anatase Ores," *Yogyo-Kyokai-Shi*, **96**(11), 1109 (1988).

Fujiki, Y., and T. Ohsaka, "Hydration and Derivatives of Potassium Dititanate Fiber," *Yogyo-Kyokai-Shi*, **90**, 19 (1982).

Fujishiro, Y., S. Uchida, and T. Sato, "Photocatalytic Hydrogen Evolution with Fibrous Titania Prepared by the Solvothermal Reactions of Protonic Layered Tetratitanate ($H_2Ti_4O_9$)," *Int. J. Inorg. Chem.*, **2**, 325 (2000).

Inoue, Y., T. Kubokawa, and K. Sato, "Photocatalytic Activity of Alkali–Metal Titanates Combined with Ruthenium in the Decomposition of Water," *J Phys Chem.*, **95**, 4059 (1991).

Johnson, J. W., R. H. Oelkers, and H. C. Helgeson, "Supcrt92: A Software Package for Calculating the Standard Molal Thermodynamic Properties of Minerals, Gases, Aqueous, and Reactions from 1 to 5000 bar and 0 to 1000°C," *Computers & Geosci.*, **18**, 899 (1992).

Karapemjants, M. Kh., and M. L. Karapemjants, *Principle of Thermodynamics: Organic and Inorganic Compounds*, Chemical Press, Moscow, USSR (1968).

Khakonov, A. I., "Determination of the Enthalpy of Formation of Titanium (IV) Hydroxide," *J. Phys. Chem. (USSR)*, **48**(6), 1552 (1974).

Kudo, A., and K. Kaneap, "Photoluminescent Properties of Ion-Exchangeable Layered Oxides," *Micropor. Mesopor. Mater.*, **21**, 615 (1998).

Kudo, A., and E. Kaneko, "Photochemical Host–Guest Interaction in Tb^{3+} and Eu^{3+} Ion-Exchanged $K_{2-x}H_xTi_2O_5$ Layered Oxides," *Chem. Commun.*, 349 (1997b).

Kudo, A., and T. Kondo, "Photoluminescent and Photocatalytic Properties of Layered Caesium Titanates, $Cs_2Ti_nO_{2n+1}$ (n = 2, 5, 6)," *J. Mater. Chem.*, **5**, 777 (1997a).

Kudo, A., and T. Sakata, "Photoluminescence of Layered Alkali–Metal Titanates ($A_2Ti_nO_{2n+1}$, A = Na,K)," *J. Mater. Chem.*, **3**(10), 1081 (1993).

Lencka, M. M., A. Anderko, and R. E. Riman, "Hydrothermal Precipitation of Lead Zirconate Titanate Solid Solutions: Thermodynamic Modeling and Experimental Synthesis," *J. Am. Ceram Soc.*, **78**, 2609 (1995).

Lencka, M. M., and R. E. Riman, "Thermodynamic Modeling of Hydrothermal Synthesis of Ceramic Powder," *Chem. Mater.*, **5**, 61 (1993a).

Lencka, M. M., and R. E. Riman, "Synthesis of Lead Titanate: Thermodynamic Modeling and Experimental Verification," *J. Am. Ceram. Soc.*, **76**, 2649 (1993b).

Masaki, N., S. Uchida, H. Yamane, and T. Sato, "Hydrothermal Synthesis of Potassium Titanates in Ti-KOH-H_2O System," *J. Mater. Sci.*, **35**, 3307 (2000).

Narita, Y., and H. Konnai, "Potassium Titanate Whisker," *Zeoraito*, **9**(3), 103 (1992).

Ogawa, M., and K. Kuroda, "Photofunctions of Intercalation Compounds," *Chem. Rev.*, **95**, 399 (1995).

Sasaki, T., M. Watanabe, Y. Fujiki, and Y. Kitami, "Synthesis, Structural Characterizations, and Some Chemical Properties of a Fibrous Titanate with a Novel Layer/Tunnel Intergrown Structure," *Chem. Mater.*, **6**, 1749 (1994).

Schaak, R. E., and T. E. Mallouk, "Perovskites by Design: A Toolbox of Solid-State Reactions," *Chem. Mater.*, **14**, 1455 (2002).

Shibata, M., A. Kudo, A. Tanaka, and K. Domen, "Photocatalytic Activities of Layered Titanium Compounds and Their Derivatives for H_2 Evolution from Aqueous Methanol Solution," *Chem. Lett.*, 1017 (1987).

Shimizu, T., "Potassium Titanate Fibers," *Ind. Chem. Jpn.*, **5**, 87 (1980); **7**, 104 (1980).

Smith, J. M., and H. C. Van Ness, *Introduction to Chemical Engineering Thermodynamics*, 3rd Edition, McGraw-Hill, Kogakusha, Japan (1975).

Stull, D. R., and H. Prophet, *JANAF Thermochemical Tables*, 2nd Edition, Nat. Stand. Ref. Data Ser. Nat. Bur. Stand. (U.S.), Washington, DC, p. 37 (1971).
Uchida, S., N. Masaki, and T. Sato, "Synthesis of a New Potassium Titanate, $KTiO_2(OH)$ by Hydrothermal Oxidation of Ti," *High Pressure Res.*, **20**, 1 (2001).
Yagi, M., and M. Kaneko, "Molecular Catalysts for Water Oxidation," *Chem. Rev.*, **101**, 21 (2001).
Yahya, R. B., H. Hayashi, T. Nagase, T. Ebina, Y. Onodera, and N. Saitoh, "Hydrothermal Synthesis of Potassium Hexatitanates under Subcritical and Supercritical Water Conditions and Its Application in Photocatalysis," *Chem. Mater.*, **13**, 842 (2001).
Yin, S., and T. Sato, "Photocatalytic Hydrogen Evolution with Fibrous Titania Prepared by the Solvothermal Reactions of Protonic Layered Tetratitanate ($H_2Ti_4O_9$)," *Ind. Eng. Chem. Res.*, **39**, 4526 (2000).

Manuscript received Jun. 6, 2003, revision received Aug. 28, 2003, and final revision received Dec. 19, 2003.